Postprint of: Malikan, M, Eremeyev, VA. Flexomagnetic response of buckled piezomagnetic composite nanoplates. COMPOSITE STRUCTURES (2021), 113932 DOI: 10.1016/j.compstruct.2021.113932

Flexomagnetic response of buckled piezomagnetic composite nanoplates

Mohammad Malikan[1], Victor A. Eremeyev[1,2,3]*

[1] Department of Mechanics of Materials and Structures, Gdansk University of Technology,80-233 Gdansk, Poland,

[2] Research and Education Center "Materials" Don State Technical University, Gagarina sq., 1, 344000 Rostov on Don, Russia,

[3] DICAAR, Università degli Studi di Cagliari, Via Marengo, 2, 09123, Cagliari, Italy

*Corresponding author:
Email: victor.eremeev@pg.edu.pl, eremeyev.victor@gmail.com

Abstract

In this paper, the equation governing the buckling of a magnetic composite plate under the influence of an in-plane one-dimensional magnetic field, assuming the concept of flexomagnetic and considering the resulting flexural force and moment, is investigated for the first time by different analytical boundary conditions. To determine the equation governing the stability of the plate, the nonlocal strain gradient theory has been used by taking into account the classical plate theory. The axial magnetic force, which is originated from the magnetic field, is investigated. After extracting the governing differential equation, the critical

buckling load is obtained for different support conditions. The effect of nonlocal parameter, sheet aspect ratio and the effect of one-dimensional magnetic field on critical load are discussed. It was earned that if the nanoplate is rectangular so that the value of aspect ratio is less than one, the flexomagnetic response will be more noticeable.

Keywords: Composite plate; Flexomagnetic; Critical buckling load; Nonlocal strain gradient theory; Analytical solution

Symbols

H_x, H_y, H_z Magnetic field components
η_{xxz} Gradient of the axial strain
η_{yyz} Gradient of the lateral strain
σ_{xx} Axial stress component
σ_{yy} Lateral stress component
σ_{xy} Shear stress component
ε_{xx} Axial strain component
ε_{yy} Lateral strain component
ε_{xy} Shear strain component
ξ_{xxz} Hyper axial stress
ξ_{yyz} Hyper lateral stress
B_z Transverse magnetic flux component
U Strain energy
δ Symbol of variation
Ψ Magnetic potential
m Mode number
μ Nonlocal parameter
a Length of the plate
b Width of the plate
h Thickness of the plate
W Work done by external factors
u_1 Cartesian displacement along x axis
u_2 Cartesian displacement along y axis
u_3 Cartesian displacement along z axis
u Displacement of the midplane along x
v Displacement of the midplane along y
w Transverse displacement of the midplane
x, y, z Length, width, and thickness coordinates
$\bar{q}_{31}, \bar{q}_{15}$ Components of the third-order piezomagnetic tensor
g_{14}, g_{15} Components the sixth-order gradient elasticity tensor
f_{14}, f_{15} Components of fourth-order flexomagnetic
$\bar{d}_{11}, \bar{d}_{33}$ Components of the second-order magnetic permeability tensor
N_{xx}^0, N_{yy}^0, N_{xy}^0 Initial total in-plane axial force
ψ Initial Magnetic potential
X_m, Y_n Residues in the solution method
$\bar{C}_{11}, \bar{C}_{22}, \bar{C}_{12}, \bar{C}_{44}, \bar{C}_{66}$ Elasticity constants
l Length scale strain gradient parameter
T_{xxz}, T_{yyz} Hyper stress resultants
N_{xx}, N_{yy}, N_{xy} Axial stress resultants
M_{xx}, M_{yy}, M_{xy} Moment stress resultants

1 Introduction

The main characteristic of magneto-electro-elastic materials is the magneto-electric effect. This effect makes mechanical, electrical, and magnetic energies convertible to each other. Like the piezoelectric layers, magneto-elastic layers can be used to control the structure. Because, magneto-electro-elastic materials have the ability to convert energy between three electric, mechanical, and magnetic fields, these materials have direct applications in sensors and actuators, vibration control in structures, and so on. Their magneto-electro-elastic correlation occurs through stress-strain relationships. The difference is that the magneto-elastic layers can be controlled remotely by applying a magnetic field to the mechanical response of the structure.

Magnetic nanosheets (MNSs) are classified into small size particles handled by the aid of a magnetic field. These elements regularly include magnetic parts in the macro scale, for instance, cobalt, nickel, iron, and their mixtures. MNSs are commonly in the range of 5-500 nanometers in thickness or diameter. Many MNSs have recently been studied due to their marvelous potential features. Optical filters, catalysts consisting of nanoparticles, and semiconductors can be a few examples of using MNSs [1-6].

In response to mechanical impact, the magnetization and/or polarization can physically appear into materials as a result of flexo-effect. It is worth to underline that polarization leads to piezoelectric [7-15] or flexoelectric [16-31] effects and magnetization results in piezomagnetic [32-40] and flexomagnetic [41-47] impacts. The piezoelectric and piezomagnetic properties resulted from the elastic strain, but the flexoelectric and flexomagnetic come from the gradient of elastic strain. In a general definition, elastic stress gradient induces magnetization in centrosymmetric magnetic materials that this concept is described as the direct flexomagnetic effect which may be exhibited in a linear behavior. Reversely, the flexomagnetic effect occurs when the magnetic field gradient induces

magnetization in the material. The difference between piezomagnetic and flexomagnetic is not limited to the aforementioned content. Piezoelectric or piezomagnetic properties can appear in non-centrosymmetric crystallines only; however, flexomagneticity can exist in centrosymmetric structures but those without time inversion. The well-studied flexoelectricity is entirely similar to the flexomagneticity in this definition.

According to existing studies, it is observed that the flexomagnetic effect in two-dimensional media and for piezomagnetic sheets has never been studied. Not long ago, Sidhardh and Ray [41] and Zhang et al. [42] developed early studies on the flexomagnetic model of piezomagnetic nanosized one-dimensional (1D) beams. These researches presented a flexomagnetic model described by the Euler-Bernoulli thin beam approach evaluating bending properties of the material. They have applied small deformations based on the linear strains of Lagrangian. They have captured both direct and converse magnetization in regard to the one-dimensional magnetic field. To bend the beam, a uniform static force was loaded on the beam length. The load acted transversely. [41] investigated a beam with one end free and another one clamped so-called cantilever. Moreover, [42] considered several boundary conditions and showed a good evaluation in this regard. Both references include a deficiency in inspecting size and nonlocal effects. In fact, they did not figure out the effects of stress nonlocality that is significant in nanoscale. However, they have used surface effects to analyze size influences. Further growth of flexomagneticity returns to [43-47] in which the size-dependency behavior of flexomagneticity was confirmed fully. Malikan and Eremeyev [43] continued [41, 42] studies but with implementing stress-driven nonlocal elasticity while imposing the vibrational environment for the Euler-Bernoulli beam. Their formulation was performed based on the linear strains and their results were carried out by different diagrams. In another research, Malikan and Eremeyev [44] extended [43] for nonlinear natural

frequencies of a flexomagnetic model that existed in a piezomagnetic nanosized beam. In this work, the small-scale effect was fulfilled according to the nonlocal strain gradient elasticity approach. Besides the mentioned researches, in a benchmark study, Malikan and Eremeyev [45] investigated the static nonlinear bending of a piezomagnetic small size beam with the inclusion of flexomagneticity. They have combined Newton-Raphson iterative solution technique with the analytical Galerkin weighted residual method to calculate values of large deflections. Their brilliant results certified that the nonlinear bending analysis is severely applicable for the flexomagnetic response of a micro/nano-electromechanical system. Their conclusions acknowledged that the existence of flexomagnetic will lead to decreasing the deflections. Malikan et al. [46] kept up their studies in the category of flexomagneticity. This new research involved the response of post-buckling of a nanobeam containing both piezomagnetic and flexomagnetic features. Malikan et al. [47] studied the influence of porosities in several manners on an axially pressurized piezomagnetic nanoscale beam incorporating flexomagnetic effect. They have confirmed that some kinds of porosity can affect the material behavior of the flexomagnetic model.

In this research and in continuation of studies on the flexomagnetic effect, the biaxial buckling of a nanosized smart piezomagnetic composite sheet consisting of flexomagnetic property in the isotropic state has been investigated for the first time. The classical plate theory, linear magneto-elastic stress-strain law, and the nonlocal strain gradient theory have been used to calculate the biaxial stability of the nanosheet. The characteristic equation was derived using Hamilton's principle and Lagrangian strain considering von Kármán hypothesis. To make the numerical outputs further certain, our results are compared with the available molecular dynamics simulations in a simple case. Numerical results are presented analytically and graphically using the solution of the Galerkin integral method. Attempts have

been made to include two boundary conditions, clamped and simply-supported, in the evaluations.

2 The Problem Modeling

As shown in Figure 1, consider a piezomagnetic nanoplate with *a*, *b*, and *h* as its length, width, and thickness, respectively. The magneto-elastic material features are dedicated to this sheet. The plate is affected by the magnetic potential resulted from the one-dimensional magnetic field. The plate is supposed to be square/rectangular.

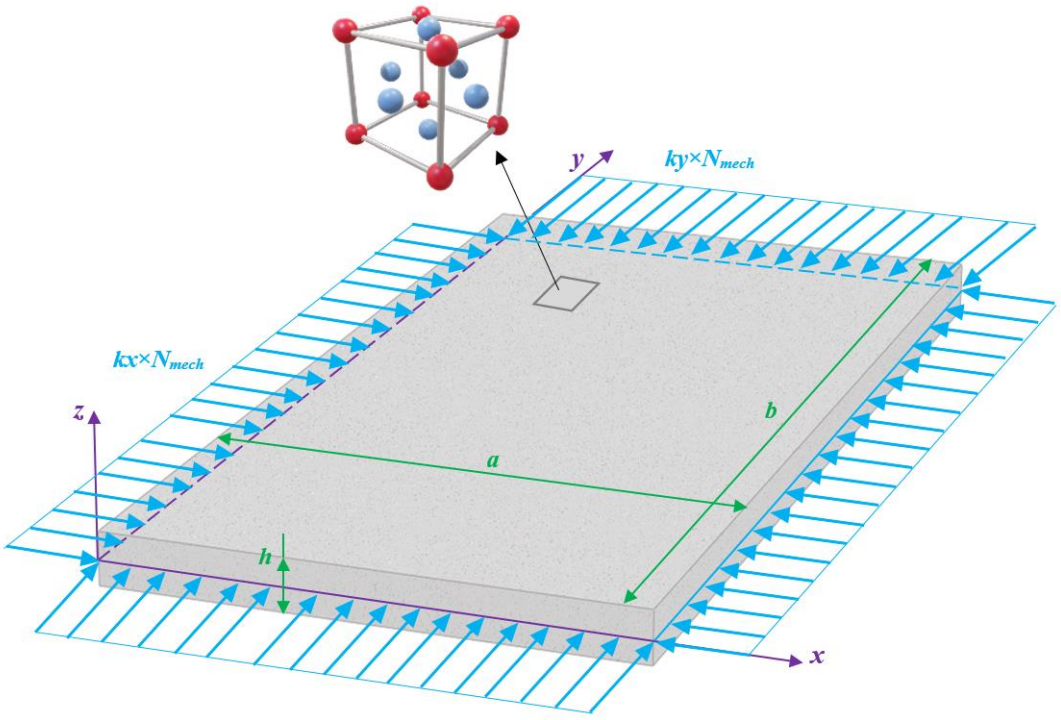

Figure 1. A square/non-square PM nanoscale plate compressed biaxially involving FM

The physical condition of the nanoplate is mathematically designed based on the classical plate theory. This is carried out as follows [48]

$$u_1(x,y,z) = u(x,y) - z\frac{\partial w(x,y)}{\partial x} \tag{1}$$

$$u_2(x,y,z) = v(x,y) - z\frac{\partial w(x,y)}{\partial y} \tag{2}$$

$$u_3(x,y,z) = w(x,y) \tag{3}$$

Using the equations of motion of the nanosheet according to the classical theory, and relations (1-3), the linear forms of strain-displacement equations are obtained in terms of non-zero displacement derivatives as follows

$$\varepsilon_{xx} = \frac{\partial u}{\partial x} - z\frac{\partial^2 w}{\partial x^2} \tag{4}$$

$$\varepsilon_{yy} = \frac{\partial v}{\partial y} - z\frac{\partial^2 w}{\partial y^2} \tag{5}$$

$$\varepsilon_{xy} = \frac{\partial u}{\partial y} + \frac{\partial v}{\partial x} - 2z\frac{\partial^2 w}{\partial x \partial y} \tag{6}$$

$$\eta_{xxz} = \frac{\partial \varepsilon_{xx}}{\partial z} = -\frac{\partial^2 w}{\partial x^2} \tag{7}$$

$$\eta_{yyz} = \frac{\partial \varepsilon_{yy}}{\partial z} = -\frac{\partial^2 w}{\partial y^2} \tag{8}$$

The constitutive relations that couple magneto-elastic properties can be expressed by tensor calculus as follows [41, 42]

$$\sigma_{ij} = C_{ijkl}\varepsilon_{kl} - q_{kij}H_k \tag{9}$$

$$\xi_{ijk} = g_{ij}\eta_{ijk} - f_{ij}H_k \tag{10}$$

$$B_i = q_{ikl}\varepsilon_{kl} + d_{ij}H_k + f_{ij}\eta_{ijk} \tag{11}$$

The Lagrangian variational principle can help find the equilibrium equations in the following

$$\delta U - \delta W = 0 \tag{12}$$

It is assumed that the magnetic field exists only in line with the transverse axis.

Therefore, the global form of the strain energy including magneto-elastic effects can be established as follows

$$\delta U = \int_V \left(\sigma_{xx}\delta\varepsilon_{xx} + \sigma_{yy}\delta\varepsilon_{yy} + +\sigma_{xy}\delta\varepsilon_{xy} + \xi_{xxz}\delta\eta_{xxz} + \xi_{yyz}\delta\eta_{yyz} - B_z\delta H_z \right) dV \tag{13}$$

Thus, as per the infinitesimal deformations, the integration by parts gives

$$\delta U = \delta\Pi_{U_1}^{Mech} + \delta\Pi_{U_1}^{Mag} + \delta\Pi_{U_2}^{Mech} + \delta\Pi_{U_2}^{Mag} \tag{14}$$

where

$$\delta\Pi_{U_1}^{Mech} = -\int_0^b \int_0^a \left[\begin{array}{l} \dfrac{\partial N_{xx}}{\partial x}\delta u + \dfrac{\partial N_{yy}}{\partial y}\delta v + \dfrac{\partial N_{xy}}{\partial x}\delta v + \dfrac{\partial N_{xy}}{\partial y}\delta u \\ + \left(\dfrac{\partial^2 M_{xx}}{\partial x^2} + \dfrac{\partial^2 M_{yy}}{\partial y^2} + 2\dfrac{\partial^2 M_{xy}}{\partial x \partial y} + \dfrac{\partial^2 T_{xxz}}{\partial x^2} + \dfrac{\partial^2 T_{yyz}}{\partial y^2} \right)\delta w \end{array} \right] dxdy \tag{15}$$

$$\delta\Pi_{U_1}^{Mag} = -\int_0^b \int_0^a \int_{-h/2}^{h/2} \frac{\partial B_z}{\partial z}\delta\Psi dz dx dy \tag{16}$$

$$\begin{array}{l} \delta\Pi_{U_2}^{Mech} = \left(\begin{array}{l} N_{xx}\delta u + N_{xy}\delta v - M_{xx}\dfrac{\partial \delta w}{\partial x} - \\ T_{xxz}\dfrac{\partial \delta w}{\partial x} + \dfrac{\partial M_{xx}}{\partial x}\delta w + \dfrac{\partial T_{xxz}}{\partial x}\delta w \end{array} \right)\Bigg|_0^a + \\ \left(\begin{array}{l} N_{yy}\delta v + N_{xy}\delta u - M_{yy}\dfrac{\partial \delta w}{\partial y} - \\ T_{yyz}\dfrac{\partial \delta w}{\partial y} + \dfrac{\partial M_{yy}}{\partial y}\delta w + \dfrac{\partial T_{yyz}}{\partial y}\delta w \end{array} \right)\Bigg|_0^b + 2M_{xy}\delta w\Big|_0^a\Big|_0^b \end{array} \tag{17}$$

$$\delta\Pi_{U_2}^{Mag} = \int_0^b \int_0^a \left(B_z\delta\Psi \right)\Big|_{-h/2}^{h/2} dxdy \tag{18}$$

The resultants of the biaxial in-plane forces, moment, and hyper stresses can be calculated by the below equations,

$$\left\{N_{xx}, N_{yy}, N_{xy}\right\} = \int_{-h/2}^{h/2} \left\{\sigma_{xx}, \sigma_{yy}, \sigma_{xy}\right\} dz \tag{19}$$

$$\left\{M_{xx}, M_{yy}, M_{xy}\right\} = \int_{-h/2}^{h/2} \left\{\sigma_{xx}, \sigma_{yy},, \sigma_{xy}\right\} z dz \tag{20}$$

$$\left\{T_{xxz}, T_{yyz}\right\} = \int_{-h/2}^{h/2} \left\{\xi_{xxz}, \xi_{yyz}\right\} dz \tag{21}$$

Due to the existence of outer loads, there would be thermodynamics work performed on the system. To determine it, we have,

$$W = -\frac{1}{2}\int_0^b \int_0^a \left\{ N_{xx}^0 \left(\frac{\partial w}{\partial x}\right)^2 + N_{yy}^0 \left(\frac{\partial w}{\partial y}\right)^2 + N_{xy}^0 \left(\frac{\partial^2 w}{\partial xy}\right)^2 \right\} dxdy \tag{22}$$

in which N_{xy}^0 shows shear in-plane force and is eliminated in this work. Hence,

$$\delta W = -\int_0^b \int_0^a \left\{ N_{xx}^0 \left(\frac{\partial w}{\partial x}\frac{\partial \delta w}{\partial x}\right) + N_{yy}^0 \left(\frac{\partial w}{\partial y}\frac{\partial \delta w}{\partial y}\right) \right\} dxdy \tag{23}$$

Let us rewrite the constitutive equation of the piezomagnetic nanoplate as follows,

$$\begin{Bmatrix} \sigma_{xx} \\ \sigma_{yy} \\ \tau_{xz} \\ \tau_{yz} \\ \tau_{xy} \end{Bmatrix} = \begin{bmatrix} \overline{C}_{11} & \overline{C}_{12} & 0 & 0 & 0 \\ \overline{C}_{12} & \overline{C}_{22} & 0 & 0 & 0 \\ 0 & 0 & \overline{C}_{44} & 0 & 0 \\ 0 & 0 & 0 & \overline{C}_{44} & 0 \\ 0 & 0 & 0 & 0 & \overline{C}_{66} \end{bmatrix} \begin{Bmatrix} \varepsilon_{xx} \\ \varepsilon_{yy} \\ \varepsilon_{xz} \\ \varepsilon_{yz} \\ \varepsilon_{xy} \end{Bmatrix} - \begin{bmatrix} 0 & 0 & \overline{q}_{31} \\ 0 & 0 & \overline{q}_{31} \\ \overline{q}_{15} & 0 & 0 \\ 0 & \overline{q}_{15} & 0 \\ 0 & 0 & 0 \end{bmatrix} \begin{Bmatrix} H_x \\ H_y \\ H_z \end{Bmatrix} \tag{24}$$

where

$$\tau_{xz} = \tau_{yz} = 0$$

In Eq. (24), the elastic and piezomagnetic properties of the nanoplate can be obtained using the following relations,

$$\begin{Bmatrix} \overline{C}_{11} \\ \overline{C}_{12} \\ \overline{C}_{44} \\ \overline{C}_{66} \end{Bmatrix} = \begin{Bmatrix} C_{11} - \dfrac{C_{13}^2}{C_{33}} \\ C_{12} - \dfrac{C_{13}^2}{C_{33}} \\ C_{44} \\ C_{66} \end{Bmatrix} \tag{25}$$

$$\begin{Bmatrix} \overline{q}_{31} \\ \overline{q}_{15} \end{Bmatrix} = \begin{Bmatrix} q_{31} - \dfrac{C_{13} q_{33}}{C_{33}} \\ q_{15} \end{Bmatrix} \tag{26}$$

And the constitutive equation of the flexomagneticity effect can be written as follows,

$$\begin{Bmatrix} \xi_{xxz} \\ \xi_{yyz} \\ \xi_{xzz} \\ \xi_{yzz} \\ \xi_{xyz} \end{Bmatrix} = \begin{bmatrix} 0 & 0 & g_{15} & 0 & 0 \\ 0 & 0 & 0 & g_{15} & 0 \\ g_{14} & g_{14} & 0 & 0 & 0 \end{bmatrix} \begin{Bmatrix} \eta_{xxz} \\ \eta_{yyz} \\ \eta_{xzz} \\ \eta_{yzz} \\ \eta_{xyz} \end{Bmatrix} - \begin{bmatrix} 0 & 0 & f_{14} \\ 0 & 0 & f_{14} \\ f_{15} & 0 & 0 \\ 0 & f_{15} & 0 \\ 0 & 0 & 0 \end{bmatrix} \begin{Bmatrix} H_x \\ H_y \\ H_z \end{Bmatrix} \tag{27}$$

in which

$$\eta_{xzz} = \eta_{yzz} = \eta_{xyz} = 0$$

$$\begin{Bmatrix} B_x \\ B_y \\ B_z \end{Bmatrix} = \begin{bmatrix} \overline{d}_{11} & 0 & 0 \\ 0 & \overline{d}_{11} & 0 \\ 0 & 0 & \overline{d}_{33} \end{bmatrix} \begin{Bmatrix} H_x \\ H_y \\ H_z \end{Bmatrix} + \begin{bmatrix} 0 & 0 & \overline{q}_{15} & 0 & 0 \\ 0 & 0 & 0 & \overline{q}_{15} & 0 \\ \overline{q}_{31} & \overline{q}_{31} & 0 & 0 & 0 \end{bmatrix} \begin{Bmatrix} \varepsilon_{xx} \\ \varepsilon_{yy} \\ \varepsilon_{xz} \\ \varepsilon_{yz} \\ \varepsilon_{xy} \end{Bmatrix} + \tag{28}$$

$$\begin{bmatrix} 0 & 0 & f_{15} & 0 & 0 \\ 0 & 0 & 0 & f_{15} & 0 \\ f_{14} & f_{14} & 0 & 0 & 0 \end{bmatrix} \begin{Bmatrix} \eta_{xxz} \\ \eta_{yyz} \\ \eta_{xzz} \\ \eta_{yzz} \\ \eta_{xyz} \end{Bmatrix}$$

in which

$$\varepsilon_{yz} = \varepsilon_{xz} = \eta_{xzz} = \eta_{yzz} = \eta_{xyz} = 0$$

$$\begin{Bmatrix} \bar{d}_{11} \\ \bar{d}_{33} \end{Bmatrix} = \begin{Bmatrix} d_{11} \\ d_{33} + \dfrac{q_{33}^2}{C_{33}} \end{Bmatrix} \tag{29}$$

The magnetic potential-component relationship can be expanded as follows,

$$H_k = \begin{Bmatrix} H_x \\ H_y \\ H_z \end{Bmatrix} = \begin{Bmatrix} -\dfrac{\partial \Psi}{\partial x} \\ -\dfrac{\partial \Psi}{\partial y} \\ -\dfrac{\partial \Psi}{\partial z} \end{Bmatrix} \tag{30}$$

To prescribe the electrical boundary conditions, one gets

$$\Psi\left(+\frac{h}{2}\right) = \psi, \ \Psi\left(-\frac{h}{2}\right) = 0 \tag{31}$$

The theoretical 1D magnetic field is supplemented by some mathematical efforts among Eqs. (18), (28), (30) and (31) as follows

$$\Psi = -\frac{\bar{q}_{31}}{2\bar{d}_{33}}\left(z^2 - \frac{h^2}{4}\right)\left(\frac{\partial^2 w}{\partial x^2} + \frac{\partial^2 w}{\partial y^2}\right) + \frac{\psi}{h}\left(z + \frac{h}{2}\right) \tag{32}$$

and then

$$H_z = z\frac{\bar{q}_{31}}{\bar{d}_{33}}\left(\frac{\partial^2 w}{\partial x^2} + \frac{\partial^2 w}{\partial y^2}\right) - \frac{\psi}{h} \tag{33}$$

Now it is possible to expand the stress field components, hyper stresses, and magnetic flux as follows

$$\begin{Bmatrix} \sigma_{xx} \\ \sigma_{yy} \\ \tau_{xy} \end{Bmatrix} = \begin{Bmatrix} \bar{C}_{11}\left(\dfrac{\partial u}{\partial x} - z\dfrac{\partial^2 w}{\partial x^2}\right) + \bar{C}_{12}\left(\dfrac{\partial v}{\partial y} - z\dfrac{\partial^2 w}{\partial y^2}\right) - \bar{q}_{31}\left(z\dfrac{\bar{q}_{31}}{\bar{d}_{33}}\left(\dfrac{\partial^2 w}{\partial x^2} + \dfrac{\partial^2 w}{\partial y^2}\right) - \dfrac{\psi}{h}\right) \\ \bar{C}_{12}\left(\dfrac{\partial u}{\partial x} - z\dfrac{\partial^2 w}{\partial x^2}\right) + \bar{C}_{22}\left(\dfrac{\partial v}{\partial y} - z\dfrac{\partial^2 w}{\partial y^2}\right) - \bar{q}_{31}\left(z\dfrac{\bar{q}_{31}}{\bar{d}_{33}}\left(\dfrac{\partial^2 w}{\partial x^2} + \dfrac{\partial^2 w}{\partial y^2}\right) - \dfrac{\psi}{h}\right) \\ \bar{C}_{66}\left(\dfrac{\partial u}{\partial y} + \dfrac{\partial v}{\partial x} - 2z\dfrac{\partial^2 w}{\partial x \partial y}\right) \end{Bmatrix} \tag{34}$$

$$\begin{Bmatrix}\xi_{xxz}\\ \xi_{yyz}\end{Bmatrix}=\begin{Bmatrix}-g_{14}\left(\dfrac{\partial^2 w}{\partial x^2}+\dfrac{\partial^2 w}{\partial y^2}\right)-f_{14}\left[z\dfrac{\bar{q}_{31}}{\bar{d}_{33}}\left(\dfrac{\partial^2 w}{\partial x^2}+\dfrac{\partial^2 w}{\partial y^2}\right)-\dfrac{\psi}{h}\right]\\ -g_{14}\left(\dfrac{\partial^2 w}{\partial x^2}+\dfrac{\partial^2 w}{\partial y^2}\right)-f_{14}\left[z\dfrac{\bar{q}_{31}}{\bar{d}_{33}}\left(\dfrac{\partial^2 w}{\partial x^2}+\dfrac{\partial^2 w}{\partial y^2}\right)-\dfrac{\psi}{h}\right]\end{Bmatrix} \tag{35}$$

$$B_z=\bar{d}_{33}\left[z\frac{\bar{q}_{31}}{\bar{d}_{33}}\left(\frac{\partial^2 w}{\partial x^2}+\frac{\partial^2 w}{\partial y^2}\right)-\frac{\psi}{h}\right]+\bar{q}_{31}\left(\frac{\partial u}{\partial x}-z\frac{\partial^2 w}{\partial x^2}+\frac{\partial v}{\partial y}-z\frac{\partial^2 w}{\partial y^2}\right)$$
$$-f_{14}\left(\frac{\partial^2 w}{\partial x^2}+\frac{\partial^2 w}{\partial y^2}\right) \tag{36}$$

Making the use of Eqs. (34-36), Eqs. (19-21) are re-written as follows

$$\begin{Bmatrix}N_{xx}\\ N_{yy}\\ N_{xy}\end{Bmatrix}=\begin{Bmatrix}A_{11}\dfrac{\partial u}{\partial x}+A_{12}\dfrac{\partial v}{\partial y}+\bar{q}_{31}\psi\\ A_{12}\dfrac{\partial u}{\partial x}+A_{22}\dfrac{\partial v}{\partial y}+\bar{q}_{31}\psi\\ A_{66}\left(\dfrac{\partial u}{\partial y}+\dfrac{\partial v}{\partial x}\right)\end{Bmatrix} \tag{37}$$

$$\begin{Bmatrix}M_{xx}\\ M_{yy}\\ M_{xy}\end{Bmatrix}=-\begin{Bmatrix}D_{11}\dfrac{\partial^2 w}{\partial x^2}+D_{12}\dfrac{\partial^2 w}{\partial y^2}\\ D_{12}\dfrac{\partial^2 w}{\partial x^2}+D_{22}\dfrac{\partial^2 w}{\partial y^2}\\ 2D_{66}\dfrac{\partial^2 w}{\partial x\partial y}\end{Bmatrix} \tag{38}$$

$$\begin{Bmatrix}T_{xxz}\\ T_{yyz}\end{Bmatrix}=\begin{Bmatrix}-g_{14}h\left(\dfrac{\partial^2 w}{\partial x^2}+\dfrac{\partial^2 w}{\partial y^2}\right)+f_{14}\psi\\ -g_{14}h\left(\dfrac{\partial^2 w}{\partial x^2}+\dfrac{\partial^2 w}{\partial y^2}\right)+f_{14}\psi\end{Bmatrix} \tag{39}$$

where

$$A_{ij}=\int_{-h/2}^{h/2}\bar{C}_{ij}dz\quad(i,j=1,2,4,6) \tag{40}$$

$$D_{ij} = \int_{-h/2}^{h/2} \left(\overline{C}_{ij} + \frac{\overline{-2}}{\overline{a}_{33}} \right) z^2 dz \quad (i, j = 1,2) \tag{41}$$

$$D_{66} = \int_{-h/2}^{h/2} \overline{C}_{66} z^2 dz \tag{42}$$

$$H_{14} = \int_{-h/2}^{h/2} g_{14} dz \tag{43}$$

Let us collect the terms in Eqs. (15) and (16) related to the governing equations, hence,

$$\frac{\partial N_{xx}}{\partial x} + \frac{\partial N_{xy}}{\partial y} = 0 \tag{44}$$

$$\frac{\partial N_{yy}}{\partial y} + \frac{\partial N_{xy}}{\partial x} = 0 \tag{45}$$

$$\frac{\partial^2 M_{xx}}{\partial x^2} + \frac{\partial^2 M_{yy}}{\partial y^2} + 2\frac{\partial^2 M_{xy}}{\partial x \partial y} + \frac{\partial^2 T_{xxz}}{\partial x^2} + \frac{\partial^2 T_{yyz}}{\partial y^2} + N_{xx}^0 \frac{\partial^2 w}{\partial x^2} + N_{yy}^0 \frac{\partial^2 w}{\partial y^2} = 0 \tag{46}$$

In the above equation, there are general biaxial compressive loads divided into two parts, mechanical and magnetic ones as follows,

$$N_{xx}^0 = k_x \times N^{Mech} + N^{Mag} \tag{47}$$

$$N_{yy}^0 = k_y \times N^{Mech} + N^{Mag} \tag{48}$$

Conforming to the Lorentz' law, one can write

$$N^{Mag} = q_{31} \psi \tag{49}$$

In mechanics, there are two general solutions to determine the strength behavior of nanostructures: 1- Laboratory methods and 2- Mathematical modeling. Since nanodimensional laboratory methods are expensive and have their own difficulties; Therefore, three main methods of mathematical modeling are considered, which are: a- Atomic modeling, b- Combined molecular and mechanical modeling, and c- Modeling based on continuum

mechanics. In terms of time constraints and the maximum number of atoms in the simulation, the first two methods are more expensive compared to modeling based on continuum mechanics, and also the unique relationships and formulations of the two methods are more complex. Therefore, this indicates that continuum mechanics can be used as a suitable solution to study physical phenomena in the field of nanotechnology.

One of the most important issues in the field of continuum mechanics is the discussion of the effects of size and its effect on the mechanical behavior of different materials. These effects will have a predominant impact on the mechanical behavior of matter when the particle size becomes very small, and theories based on classical continuum mechanics are unable to take such effects into account. This is especially evident in atomic space where the size of structures is not very large compared to the intra-atomic properties of materials. In fact, the effects of size occur due to the interaction of two scales of internal characteristic length such as distance between particles and external characteristic length such as crack length. One of the generalized theories of continuum mechanics that study such a phenomenon is the theory of nonlocal elasticity of the strain gradient [49].

$$\left\{1-\mu\left(\frac{\partial^2}{\partial x^2}+\frac{\partial^2}{\partial y^2}\right)\right\}\sigma_{ij}=C_{ijkl}\left\{1-l^2\left(\frac{\partial^2}{\partial x^2}+\frac{\partial^2}{\partial y^2}\right)\right\}\varepsilon_{kl} \tag{50}$$

In the absence of thickness effect ($\partial/\partial z$) on Eq. (50), Eqs. (37-39) shall be rewritten in terms of Eq. (50) as [50-55],

$$\left\{1-\mu\left(\frac{\partial^2}{\partial x^2}+\frac{\partial^2}{\partial y^2}\right)\right\}\begin{Bmatrix}N_{xx}\\N_{yy}\\N_{xy}\end{Bmatrix}=\left\{1-l^2\left(\frac{\partial^2}{\partial x^2}+\frac{\partial^2}{\partial y^2}\right)\right\}\begin{Bmatrix}A_{11}\dfrac{\partial u}{\partial x}+A_{12}\dfrac{\partial v}{\partial y}+\bar{q}_{31}\psi\\A_{12}\dfrac{\partial u}{\partial x}+A_{22}\dfrac{\partial v}{\partial y}+\bar{q}_{31}\psi\\A_{66}\left(\dfrac{\partial u}{\partial y}+\dfrac{\partial v}{\partial x}\right)\end{Bmatrix} \tag{51}$$

$$\left\{1-\mu\left(\frac{\partial^2}{\partial x^2}+\frac{\partial^2}{\partial y^2}\right)\right\}\begin{Bmatrix}M_{xx}\\M_{yy}\\M_{xy}\end{Bmatrix}=-\left\{1-l^2\left(\frac{\partial^2}{\partial x^2}+\frac{\partial^2}{\partial y^2}\right)\right\}\begin{Bmatrix}D_{11}\dfrac{\partial^2 w}{\partial x^2}+D_{12}\dfrac{\partial^2 w}{\partial y^2}\\D_{12}\dfrac{\partial^2 w}{\partial x^2}+D_{22}\dfrac{\partial^2 w}{\partial y^2}\\2D_{66}\dfrac{\partial^2 w}{\partial x\partial y}\end{Bmatrix} \tag{52}$$

$$\left\{1-\mu\left(\frac{\partial^2}{\partial x^2}+\frac{\partial^2}{\partial y^2}\right)\right\}\begin{Bmatrix}T_{xxz}\\T_{yyz}\end{Bmatrix}=\left\{1-l^2\left(\frac{\partial^2}{\partial x^2}+\frac{\partial^2}{\partial y^2}\right)\right\}\begin{Bmatrix}-H_{14}\left(\dfrac{\partial^2 w}{\partial x^2}+\dfrac{\partial^2 w}{\partial y^2}\right)+f_{14}\psi\\-H_{14}\left(\dfrac{\partial^2 w}{\partial x^2}+\dfrac{\partial^2 w}{\partial y^2}\right)+f_{14}\psi\end{Bmatrix} \tag{53}$$

If we compare the *x*-*y* in-plane magnetic field and deformations with those in line with thickness, then the in-plane derivatives can be eliminated. Thus, by means of Eqs. (46) and (51-53), the characteristic equation of buckling of the PM nanocomposite plate representing FM, can be simplified as follows,

$$\begin{aligned}&-\left(D_{11}+H_{14}+\mu N_{xx}^0\right)\frac{\partial^4 w}{\partial x^4}-\left[2D_{12}+4D_{66}+2H_{14}+\mu\left(N_{xx}^0+N_{yy}^0\right)\right]\\&\times\frac{\partial^4 w}{\partial x^2\partial y^2}-\left(D_{22}+H_{14}+\mu N_{yy}^0\right)\frac{\partial^4 w}{\partial y^4}+N_{xx}^0\frac{\partial^2 w}{\partial x^2}+N_{yy}^0\frac{\partial^2 w}{\partial y^2}+\\&l^2\left\{\begin{aligned}&\left[\left(D_{11}+H_{14}\right)\frac{\partial^6 w}{\partial x^6}+\left(D_{11}+2D_{12}+4D_{66}+3H_{14}\right)\frac{\partial^6 w}{\partial x^4\partial y^2}\right]\\&+\left(D_{22}+2D_{12}+4D_{66}+3H_{14}\right)\frac{\partial^6 w}{\partial x^2\partial y^4}+\left(D_{22}+H_{14}\right)\frac{\partial^6 w}{\partial y^6}\end{aligned}\right\}=0\end{aligned} \tag{54}$$

3 Solving approach

3.1 Analytical process

The solution of Eq. (54) gives the numerical values of critical buckling loads for the PM-FM nanocomposite plate. This section supplements an analytical process in conjunction with the

two analytical boundary/edge conditions that are simply supported and clamped. The essential and natural edge conditions can be mentioned as follows,

Simply-supported (S):

$$w\,(0, y) = w\,(a, y) = 0 \tag{55a}$$

$$w\,(x, 0) = w\,(x, b) = 0 \tag{55b}$$

$$M_x\,(x, 0) = M_x\,(x, b) = 0 \tag{56a}$$

$$M_y\,(0, y) = M_y\,(a, y) = 0 \tag{56b}$$

Clamped (C):

$$w\,(0, y) = w\,(a, y) = 0 \tag{57a}$$

$$w\,(x, 0) = w\,(x, b) = 0 \tag{57b}$$

The closed-form approximate function is devoted to applying the analytical solution as follows,

$$w = \sum_{m=1}^{\infty}\sum_{n=1}^{\infty} W_{mn} X_m(x) Y_n(y) \tag{58}$$

The natural and essential conditions mentioned by Eqs. (55-57) can be satisfied by the next equation in which the admissible functions are demonstrated by Table 1 [33, 56],

$$\int_0^a \int_0^b \left(w \times X_m(x) Y_n(y)\right) dy dx \tag{59}$$

Table 1. Simply-supported and clamped analytical boundary conditions for plates

Analytical edge conditions						
Notation	$x=0$	$y=0$	$x=a$	$y=b$	$X_m(x)$	$Y_n(y)$
SSSS	S	S	S	S	$\sin\left(\frac{\pi}{a}x\right)$	$\sin\left(\frac{\pi}{b}y\right)$

CCCC	C	C	C	C	$\sin^2\left(\frac{\pi}{a}x\right)$	$\sin^2\left(\frac{\pi}{b}y\right)$

3.2 Solution validity

To validate the proposed model, the isotropic nanosheet without piezo-flexomagnetic properties is considered and its critical load is shown and tabulated in Table 2 for the values provided for the simple boundary conditions and various values of length and width. The solution method is tested through molecular dynamics [57] and a good agreement can be seen. E=1TPa, υ=0.3, h=0.34 nm, μ=1.85nm^2, l=0, β=a/b=1, k_1=1, k_2=1, SSSS [57]

Table 2. A fully simply-supported nanoplate compressed biaxially

Critical buckling load ($Pa.m$)		
Present (CPT)	MD [57]	a=b
1.1570	1.0837	4.99
0.6979	0.6536	8.080
0.4658	0.4331	10.77
0.2829	0.2609	14.65
0.1874	0.1714	18.51
0.1325	0.1191	22.35
0.0981	0.0889	26.22
0.0756	0.0691	30.04
0.0601	0.0554	33.85
0.0484	0.0449	37.81

4 Discussion and results

In this section, the importance of the flexomagnetic property will be evaluated in detail by changing important and key parameters, and we will find the conditions during which this effect manifests itself most. First, the magneto-elastic properties of the sheet are presented in Table 3 [33, 41, 42]. Variable parameters are expressed below each figure.

Table 3. Magneto-elastic constants for the proposed PM-FM $CoFe_2O_4$ nanoplate

C_{11}= C_{22}=226GPa, C_{12}=125GPa, C_{13}=124GPa,
C_{33}=216GPa, C_{44}=44.2GPa, C_{66}=50.5GPa,
f_{31}=10^{-9} N/A
q_{31}=290.1 N/A.m, q_{33}=349.9 N/A.m
d_{33}=83.5×10^{-6} N/A^2

The most important problem in terms of micro/nanoscale discussions is nothing but determining the amount of nonlocal and strain gradient length scale (SGLS) parameters. Some researchers found that these factors shall not have constant values and are dependent on several objects [58, 59]. In the case of SGLS, [59] indicated that geometrical sizes, particularly thickness has strongly affected the value of SGLS. However, in the matter of values of the nonlocal parameter, the effective factors influenced it, can be the type of boundary conditions. On that account, in this part, we realize the values of SGLS concerning the thickness of the plate and the values of the nonlocal parameter with reference to the previous works between 0-2 nm.

More importantly, in most figures, the behavior of the plate in the uniaxial compression mode is compared to that of the two-axis. The sheet will have an isotropic behavior and therefore no difference in the square state if the axial load of the uniaxial axis is longitudinal or lateral. Abbreviated terms such as PFM and PM define the sheet with piezomagnetic-flexomagnetic and piezomagnetic properties, respectively. Magnetic potential values are obtained in milli-Amperes, which in turn indicates the greater importance of the magnetic field at the nanoscale. The β parameter has also been used to determine the length to width ratio (aspect ratio).

Figures 2a and 2b show how changes in the SGLS will affect the flexomagnetic properties of the sheet. The first argument that the appearance of the two figures shows can be

the greater difference between PM and PFM results in uniaxial buckling. This means that if the magnetic sheet is subjected to in-plane loading of buckling in only one direction, its flexomagnetic property will be greater. As it turns out, the increasing slope of the critical load results from increasing the SGLS parameter for the CCCC boundary conditions is greater than the SSSS ones. This excess is also more obtained for uniaxial buckling. On the other hand, comparing the results of the two boundary conditions proves that the flexomagnetic effect is greater for the CCCC quadrilateral plate than the SSSS one. The last conclusion from these figures can be the impact of SGLS on the flexomagnetic response of the nanoplate. When l/h=0 which means we eliminate the SGLS, the PFM/PM result for the uniaxial case would be 1.069 and for l/h=1, it would be 1.070. These differences confirm that the larger the SGLS parameter values, the bit more emphasize the flexomagnetic property.

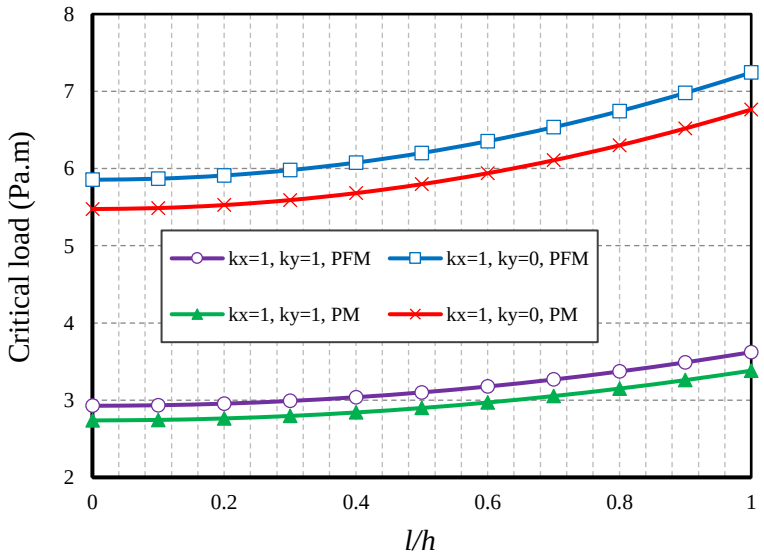

Fig. 2a. SGLS parameter vs. critical load of buckling (ψ=1mA, e_0a=1nm, β=1, b/h=15, CCCC)

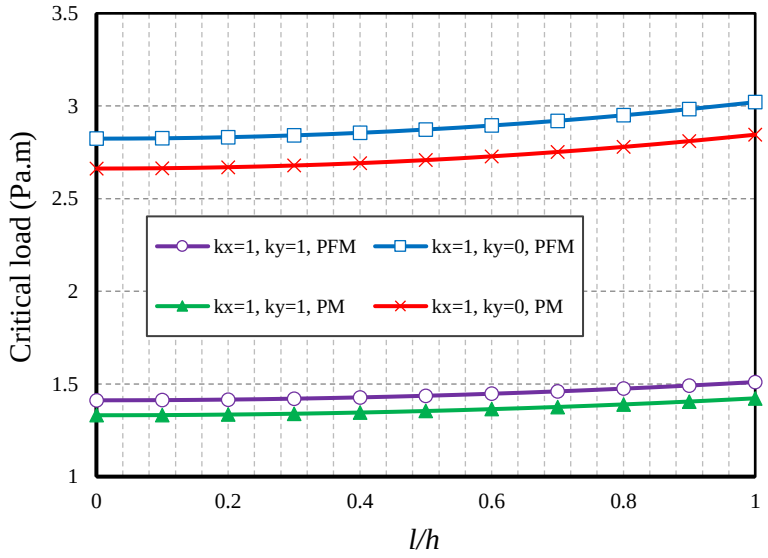

Fig. 2b. SGLS parameter vs. critical load of buckling (ψ=1mA, e_0a=1nm, β=1, b/h=15, SSSS)

After examining Figures 2a and 2b and obtaining some important results, with the help of Figures 3a and 3b we will investigate the effect of changes in the nonlocal parameter. The effect of this parameter, as has been proved many times, is a reducing effect on the stiffness of the material, and therefore increasing it here will lead to reducing the critical load. According to these two figures, we can say that if the numerical value of the nonlocal parameter is large, in both uniaxial and biaxial buckling, we will see the results of the PM and PFM approach to each other. As a result, it can be stated that nonlocality will have a considerable effect on flexomagnetic behavior. However, unlike the SGLS parameter, which has a positive effect on the flexomagnetic behavior of the sheet, the nonlocal parameter will have a negative effect and leads to less importance of this magneto-elastic property of the material.

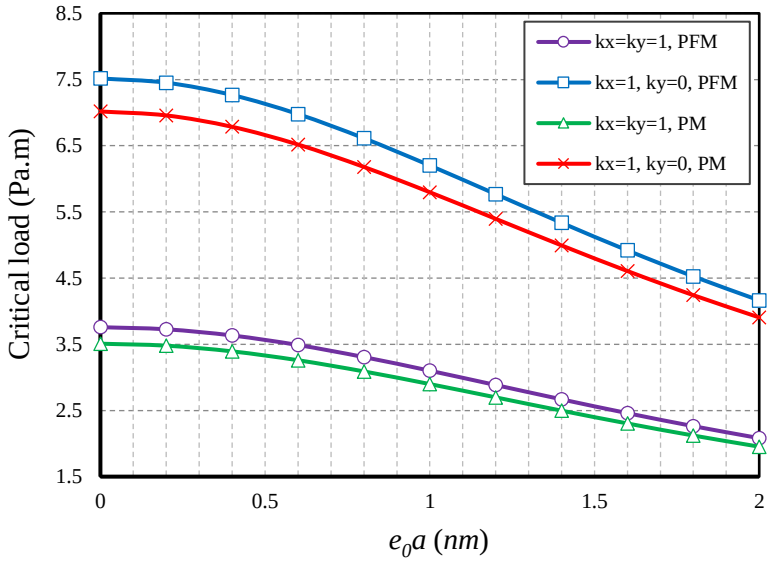

Fig. 3a. Nonlocal parameter vs. critical load of buckling in two states of magnetic (ψ=1mA, l=0.5h, b/h=15, β=1, CCCC)

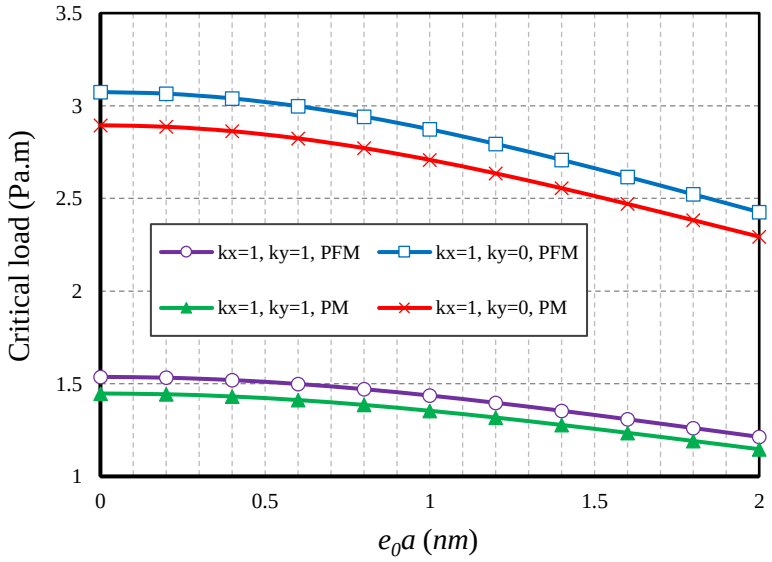

Fig. 3b. Nonlocal parameter vs. critical load of buckling in two states of magnetic (ψ=1mA, l=0.5h, b/h=15, β=1, SSSS)

Although the effect of the magnetic potential will be more predictable due to the application of a linear magnetic field, its study is not without merit. Figures 4a and 4b deal with this issue. By observing these two diagrams, it can be seen that if the sheet is subjected to

uniaxial buckling, it will be more affected by the magnetic field. In general, increasing the numerical values of the magnetic potential will increase the stiffness of the material, but this is more the case in uniaxial buckling than in the biaxial one. The interesting thing about these two figures is that if the potential of the magnetic field is negative, the critical load of the PM plate will be greater than that of the PFM sheet. As a result, the positive or negative potential of the magnetic field indicates that the PM or PFM material is stiffer.

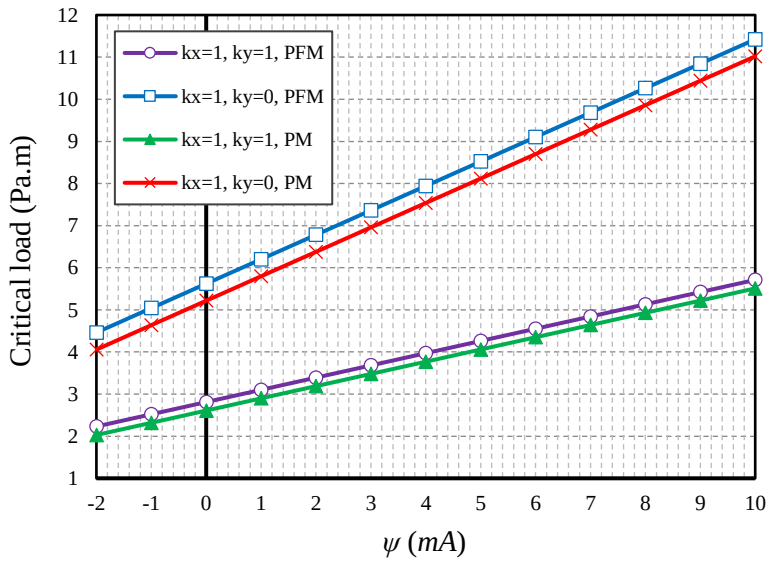

Fig. 4a. Magnetic potential vs. critical load of buckling in two states of magnetic (e_0a=1nm, l=0.5h, b/h=15, β=1, CCCC)

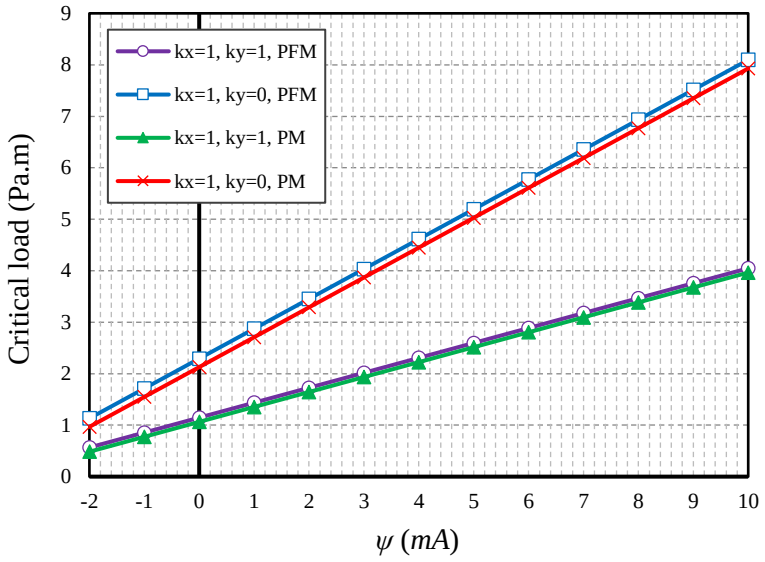

Fig. 4b. Magnetic potential vs. critical load of buckling in two states of magnetic (e_0a=1nm, l=0.5h, b/h=15, β=1, SSSS)

In the continuation of the discussion and results, we would like to examine the rectangularity of the sheet and its effect on the flexomagnetic response of the material. According to Figures 5a and 5b, we see that increasing the β coefficient leads to a reduction of the critical load and the overall stiffness of the material, which is true in both boundary conditions. But the most important result that can be found from these two figures is that in the case of a rectangular nanoplate, if the values of β are greater than 1, the results of PM are closer to the results of PFM, and this will increase with more amount of β. Rectangular nanosheets with a large value of β coefficient will not have a significant flexomagnetic effect. However, if the value of aspect ratio is less than 1, although the sheet is rectangular, the difference between the results of the PM plate and the PFM one is remarkable.

Figures 6a and 6b are plotted to examine the results of Figures 5a and 5b for uniaxial buckling. It is interesting that when the critical buckling load is applied uniaxially on the sheet, before β=1, the critical load has a decreasing behavior, but after β=1, the critical load results

will have an increasing trend. Perhaps the physical reason is that because the uniaxial critical load is applied along the x-axis, and since β greater than 1 means that the longitudinal dimension of the nanoplate is larger, then increasing the value of aspect ratio will increase the critical load.

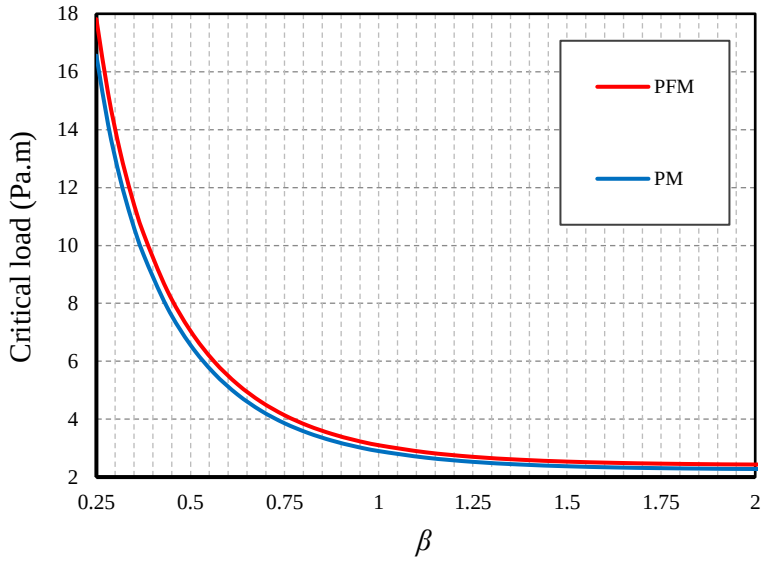

Fig. 5a. Aspect ratio vs. critical load of biaxial buckling in two states of magnetic (ψ=1mA, l=0.5h, e_0a=1nm, b/h=15, CCCC)

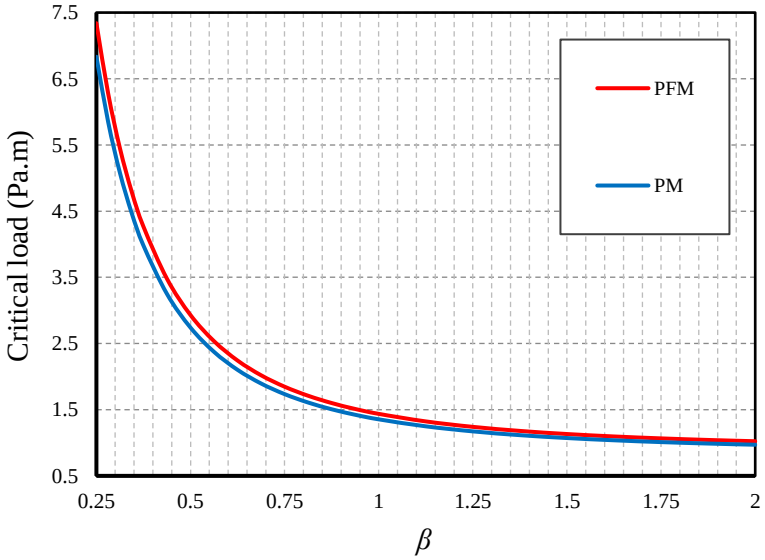

Fig. 5b. Aspect ratio vs. critical load of biaxial buckling in two states of magnetic (ψ=1mA, l=0.5h, e_0a=1nm, b/h=15, SSSS)

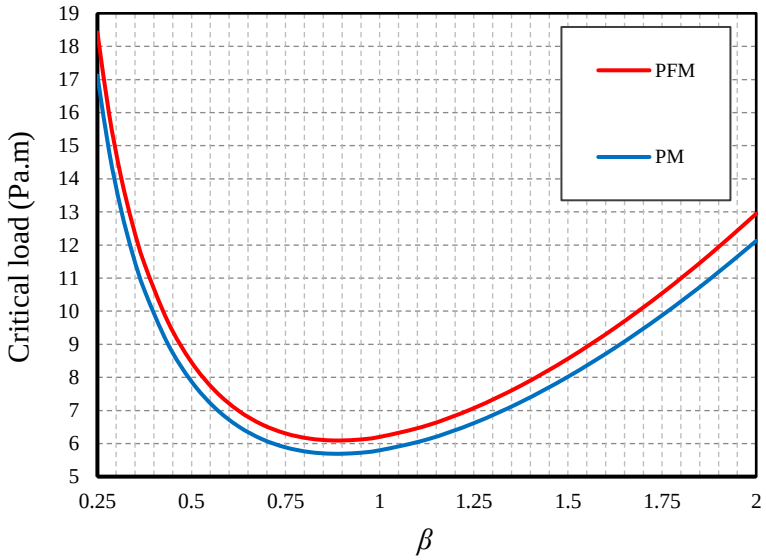

Fig. 6a. Aspect ratio vs. critical load of uniaxial buckling in two states of magnetic (ψ=1mA, l=0.5h, e_0a=1nm, b/h=15, k_x=1, k_y=0, CCCC)

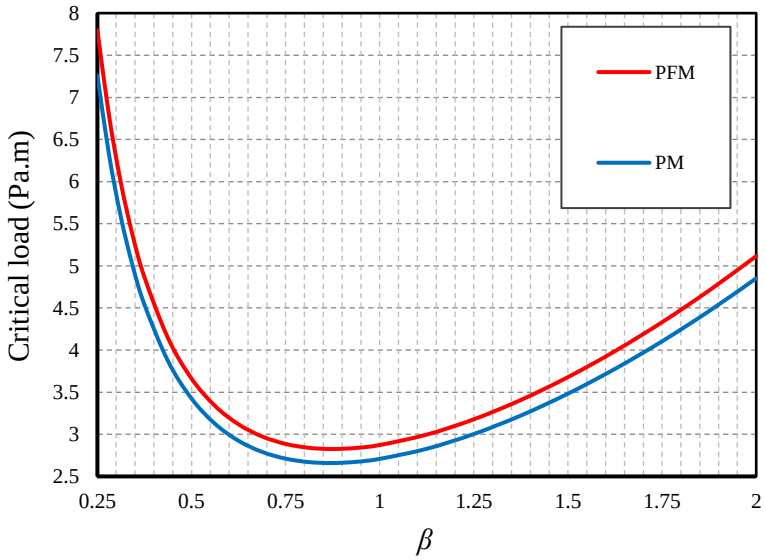

Fig. 6b. Aspect ratio vs. critical load of uniaxial buckling in two states of magnetic (ψ=1mA, l=0.5h, e_0a=1nm, b/h=15, k_x=1, k_y=0, SSSS)

5 Conclusions

A biaxial buckling analysis-based mathematical modeling was depicted for converse flexomagnetic influence on a piezomagnetic nanoparticle composition of cobalt and ferrite.

The equation of motion was obtained based on the classical plate theory and plane strain assumptions. And after the analytical solution of the equation, the analytical relation was obtained for the first mode of the buckling load of this sheet based on the clamped and simply-supported edge conditions. A MATLAB code was written to calculate the 2D domain flexomagneticity response. The following results are obtained by providing some examples and due to varying in values of fundamental parameters:

- The uniaxial buckling makes the flexomagnetic response of the nanoplate more notable.
- For the case of uniaxial buckling, the magnetic field has affected further the critical buckling load.
- In terms of biaxial buckling, while $\beta<1$, the flexomagnetic response is more obvious in contrast to $\beta>1$.
- Under uniaxial loading, whenever the nanoplate is rectangular and $\beta<1$, an increase of aspect ratio leads to softening and this is vice versa for rectangular nanoplate with $\beta>1$.

Data availability

The raw/processed data required to reproduce these findings cannot be shared at this time as the data also forms part of an ongoing study.

Acknowledgements

V.A.E acknowledges the support of the Government of the Russian Federation (contract No. 14.Z50.31.0046).

References

[1] A. H. Lu, W. Schmidt, N. Matoussevitch, H. Bönnemann, B. Spliethoff, B. Tesche, E.

Bill, W. Kiefer, F. Schüth, Nanoengineering of a Magnetically Separable Hydrogenation, Catalyst, Angewandte Chemie International, 43 (2004) 4303–4306.

[2] A. K. Gupta, M. Gupta, Synthesis and surface engineering of iron oxide nanoparticles for biomedical applications, Biomaterials, 26 (2005) 3995–4021.

[3] S. Mornet, S. Vasseur, F. Grasset, P. Verveka, G. Goglio, A. Demourgues, J. Portier, E. Pollert, E. Duguet, Magnetic nanoparticle design for medical applications, Progress in Solid State Chemistry, 34 (2006) 237-247.

[4] B. Gleich, J. Weizenecker, Tomographic imaging using the nonlinear response of magnetic particles, Nature, 435 (2005) 1214–1217.

[5] J. Philip, T. J. Kumar, P. Kalyanasundaram, B. Raj, Tunable Optical Filter, Measurement Science & Technology, 14 (2003) 1289–1294.

[6] C. Wang, M. Ge, J. Z. Jiang, Magnetic behavior of SnO2 nanosheets at room temperature, Applied Physics Letters, 97 (2010) 042510.

[7] Ch. Sun, J. Shi, X. Wang, Fundamental study of mechanical energy harvesting using piezoelectric nanostructures, Journal of Applied Physics, 108 (2010) 034309.

[8] X.-Q. Fang, J.-X. Liu, V. Gupta, Fundamental formulations and recent achievements in piezoelectric nano-structures: a review, Nanoscale, 5 (2013) 1716-1726.

[9] A. A. Girchenko, V. A. Eremeyev, N. F. Morozov, Modeling of spiral nanofilms with piezoelectric properties, Physical Mesomechanics, 14 (2011) 10-15.

[10] V. A. Eremeev, A.V. Nasedkin, Natural vibrations of nanodimensional piezoelectric

bodies with contact-type boundary conditions, Mechanics of Solids, 50 (2015) 495–507.

[11] J. Chróścielewski, R. Schmidt, V. A. Eremeyev, Nonlinear finite element modeling of vibration control of plane rod-type structural members with integrated piezoelectric patches, Continuum Mechanics and Thermodynamics, 31 (2019) 147–188.

[12] M. Malikan, Electro-mechanical shear buckling of piezoelectric nanoplate using modified couple stress theory based on simplified first order shear deformation theory, Applied Mathematical Modelling, 48 (2017) 196-207.

[13] M. Malikan, Temperature influences on shear stability of a nanosize plate with piezoelectricity effect, Multidiscipline Modeling in Materials and Structures, 14 (2018) 122-142.

[14] M. Malikan, Electro-thermal buckling of elastically supported double-layered piezoelectric nanoplates affected by an external electric voltage, Multidiscipline Modeling in Materials and Structures, 15 (2019) 50-78.

[15] H. M Sedighi, M. Malikan, A. Valipour, K. Kamil Żur, Nonlocal vibration of carbon/boron-nitride nano-hetero-structure in thermal and magnetic fields by means of nonlinear finite element method, Journal of Computational Design and Engineering, 7 (2020) 591–602.

[16] A. S. Yurkov, A. K. Tagantsev, Strong surface effect on direct bulk flexoelectric response in solids, Applied Physics Letters, 108 (2016) 022904.

[17] B. Wang, Y. Gu, S. Zhang, L.-Q. Chen, Flexoelectricity in solids: Progress, challenges, and perspectives, Progress in Materials Science, 106 (2019) 100570.

[18] L. Cross, Flexoelectric effects: charge separation in insulating solids subjected to elastic strain gradients, Journal of Materials Science, 41 (2006) 53–63.

[19] W. Ma, L. E. Cross, Observation of the flexoelectric effect in relaxor Pb ($Mg_{1/3}Nb_{2/3}$)O_3 ceramics, Applied Physics Letters,78 (2001) 2920–21.

[20] W. Ma, L. E. Cross, Flexoelectricity of barium titanate, Applied Physics Letters, 88 (2006) 232902.

[21] P. Zubko, G. Catalan, A. Buckley, P. R. L. Welche, J. F. Scott, Strain-gradient-induced polarization in SrTiO3 single crystals, Physical Review Letters, 99 (2007) 167601.

[22] V. A. Eremeyev, J.-F. Ganghoffer, V. Konopinska-Zmysłowska, N. S. Uglov, Flexoelectricity and apparent piezoelectricity of a pantographic micro-bar, International Journal of Engineering Science, 149 (2020) 103213.

[23] M. Esmaeili, Y. Tadi Beni, Vibration and Buckling Analysis of Functionally Graded Flexoelectric Smart Beam, Journal of Applied and Computational Mechanics, 5 (2019) 900-917. doi: 10.22055/jacm.2019.27857.1439

[24] M. Malikan, V. A. Eremeyev, On the Dynamics of a Visco–Piezo–Flexoelectric Nanobeam, Symmetry, 12 (2020) 643. https://doi.org/10.3390/sym12040643

[25] W. Ma, Flexoelectricity: strain gradient effects in ferroelectrics, Physica Scripta, T129 (2007) 180-183.

[26] D. Lee, A. Yoon, S. Y. Jang, J.-G. Yoon, J.-S. Chung, M. Kim, J. F. Scott, and T. W. Noh, Giant Flexoelectric Effect in Ferroelectric Epitaxial Thin Films, Physical Review Letters, 107 (2011) 057602.

[27] T. D. Nguyen, S. Mao, Y.-W. Yeh, P. K. Purohit, M. C. McAlpine, Nanoscale Flexoelectricity, Advanced Materials, 25 (2013) 946-974.

[28] P. Zubko, G. Catalan, A. K. Tagantsev, Flexoelectric Effect in Solids, Annual Review of Materials Research, 43 (2013) 387-421.

[29] P. V. Yudin, A. K. Tagantsev, Fundamentals of flexoelectricity in solids, Nanotechnology, 24 (2013) 432001.

[30] P. Zubko, G. Catalan, A. K. Tagantsev, Flexoelectric Effect in Solids, Annual Review of Materials Research, 43 (2013) 387–421.

[31] P. V. Yudin, A. K. Tagantsev, Fundamentals of flexoelectricity in solids, Nanotechnology, 24 (2013) 432001.

[32] M. Malikan, V. B. Nguyen, F. Tornabene, Electromagnetic forced vibrations of composite nanoplates using nonlocal strain gradient theory, Materials Research Express, 5 (2018) 075031.

[33] M. Malikan, V. B. Nguyen, Buckling analysis of piezo-magnetoelectric nanoplates in hygrothermal environment based on a novel one variable plate theory combining with higher-order nonlocal strain gradient theory, Physica E: Low-dimensional Systems and Nanostructures, 102 (2018) 8-28.

[34] M. Malikan, V. B. Nguyen, F. Tornabene, Damped forced vibration analysis of single-walled carbon nanotubes resting on viscoelastic foundation in thermal environment using nonlocal strain gradient theory, Engineering Science and Technology, an International Journal, 21 (2018) 778–786.

[35] M. Malikan, M. Krasheninnikov, V. A. Eremeyev, Torsional stability capacity of a nano-composite shell based on a nonlocal strain gradient shell model under a three-dimensional magnetic field, International Journal of Engineering Science, 148 (2020) 103210.

[36] P. Lukashev, R. F. Sabirianov, Flexomagnetic effect in frustrated triangular magnetic structures, Physical Review B, 82 (2010) 094417.

[37] E. A. Eliseev, A. N. Morozovska, V. V. Khist, V. Polinger, effective flexoelectric and flexomagnetic response of ferroics, In Recent Advances in Topological Ferroics and their Dynamics, Solid State Physics; Stamps, R. L., Schultheis, H.; Elsevier, Netherlands, 2019; Volume 70, pp. 237-289.

[38] A. F. Kabychenkov, F. V. Lisovskii, Flexomagnetic and flexoantiferromagnetic effects in centrosymmetric antiferromagnetic materials, Technical Physics, 64 (2019) 980-983.

[39] E. A. Eliseev, A. N. Morozovska, M. D. Glinchuk, R. Blinc, Spontaneous flexoelectric/flexomagnetic effect in nanoferroics, Physical Review B, 79 (2009) 165433.

[40] W. Fahrner, Nanotechnology and Nanoelectronics, 1st ed.; Springer, Germany, 2005; pp. 269.

[41] S. Sidhardh, M. C. Ray, Flexomagnetic response of nanostructures, Journal of Applied Physics, 124 (2018) 244101.

[42] N. Zhang, Sh. Zheng, D. Chen, Size-dependent static bending of flexomagnetic nanobeams, Journal of Applied Physics, 126 (2019) 223901.

[43] M. Malikan, V. A. Eremeyev, Free Vibration of Flexomagnetic Nanostructured Tubes Based on Stress-driven Nonlocal Elasticity. In Analysis of Shells, Plates, and Beams, 1st ed.; Altenbach, H., Chinchaladze, N., Kienzler R., Müller, W. H., Eds.; Springer Nature, Switzerland, 2020; Volume 134, pp. 215-226.

[44] M. Malikan, V. A. Eremeyev, On the geometrically nonlinear vibration of a piezo-flexomagnetic nanotube, Mathematical Methods in the Applied Sciences, (2020). https://doi.org/10.1002/mma.6758

[45] M. Malikan, V. A. Eremeyev, On nonlinear bending study of a piezo-flexomagnetic nanobeam based on an analytical-numerical solution, Nanomaterials, 10 (2020) 1-22. https://doi.org/10.3390/nano10091762

[46] M. Malikan, Nikolay S. Uglov, V. A. Eremeyev, On instabilities and post-buckling of piezomagnetic and flexomagnetic nanostructures, International Journal of Engineering Science, 157 (2020) Article no 103395.

[47] M. Malikan, V. A. Eremeyev, K. K. Żur, Effect of Axial Porosities on Flexomagnetic Response of In-Plane Compressed Piezomagnetic Nanobeams, Symmetry, 12 (2020) 1935.

[48] J. N. Reddy, Nonlocal nonlinear formulations for bending of classical and shear deformation theories of beams and plates, International Journal of Engineering Science, 48 (2010) 1507-1518.

[49] C. W. Lim, G. Zhang, J. N. Reddy, A Higher-order nonlocal elasticity and strain gradient theory and Its Applications in wave propagation, Journal of the Mechanics and Physics of Solids, 78 (2015) 298-313.

[50] G. L. She, H. B. Liu, B. Karami, On resonance behavior of porous FG curved nanobeams, Steel and Composite Structures, 36 (2020) 179–186.

[51] B. Karami, D. Shahsavari, M. Janghorban, L. Li, On the resonance of functionally graded nanoplates using bi-Helmholtz nonlocal strain gradient theory, International Journal of Engineering Science, 144 (2019) 103143.

[52] S. Esfahani, S. Esmaeilzade Khadem, A. Ebrahimi Mamaghani, Nonlinear vibration analysis of an electrostatic functionally graded nano-resonator with surface effects based on nonlocal strain gradient theory, International Journal of Mechanical Sciences, 151 (2019) 508-522.

[53] X. Xu, B. Karami, M. Janghorban, On the dynamics of nanoshells, International Journal

of Engineering Science, 158 (2021) 103431.

[54] M. Malikan, On the plastic buckling of curved carbon nanotubes, Theoretical and Applied Mechanics Letters, 10 (2020) 46-56.

[55] H. Sarparast, A. Ebrahimi-Mamaghani, M. Safarpour, H. M. Ouakad, R. Dimitri, F. Tornabene, Nonlocal study of the vibration and stability response of small-scale axially moving supported beams on viscoelastic-Pasternak foundation in a hygro-thermal environment, Mathematical Methods in the Applied Sciences, (2020). https://doi.org/10.1002/mma.6859

[56] M. Malikan, V. A. Eremeyev, A new hyperbolic-polynomial higher-order elasticity theory for mechanics of thick FGM beams with imperfection in the material composition, Composite Structures, 249 (2020) 112486.

[57] R. Ansari, S. Sahmani, Prediction of biaxial buckling behavior of single-layered graphene sheets based on nonlocal plate models and molecular dynamics simulations, Applied Mathematical Modelling, 37 (2013) 7338–7351.

[58] R. Ansari, S. Sahmani, B. Arash, Nonlocal plate model for free vibrations of single-layered graphene sheets, Physics Letters A, 375 (2010) 53-62.

[59] M. Akbarzadeh Khorshidi, The material length scale parameter used in couple stress theories is not a material constant, International Journal of Engineering Science, 133 (2018) 15-25.